

1
2
3
4
5
6
7
8
9
10
11
12
13
14
15
16
17
18
19
20
21
22
23
24
25
26
27
28
29
30
31
32
33
34
35
36
37
38
39
40
41
42
43
44
45
46
47

The influence of seasonality on estimating return values of significant wave height

Melisa Menéndez^{1*}, Fernando J. Méndez¹, Cristina Izaguirre¹, Alberto Luceño², Inigo J. Losada¹

¹ Ocean & Coastal Research Group, IH Cantabria, Universidad de Cantabria, Spain

² Dpto. Matemática Aplicada y Ciencias de la Computación, Universidad de Cantabria, Spain

* Corresponding author

Manuscript submitted to: Journal of Geophysical Research

Date of submission: September 13, 2007

Corresponding author address

Ocean & Coastal Research Group (Instituto de Hidráulica Ambiental "IH Cantabria"), Universidad de Cantabria.

Avda. de los Castros s/n 39005 Santander (SPAIN)

Phone: +34-942-201810

Fax: +34-942-201860

e-mail: menendezm@unican.es

Keywords

generalized extreme value, maximum likelihood, return level, seasonality, statistical model, time-dependent, wave climate

48
49
50
51
52
53
54
55
56
57
58
59
60
61
62
63
64
65
66
67
68
69
70
71
72
73
74

Abstract

A time-dependent generalized extreme value (GEV) model for monthly significant wave heights maxima is developed. The model is applied to several 3-hour time series from the Spanish buoy network. Monthly maxima show a clear non-stationary behavior within a year, suggesting that the location, scale and shape parameters of the GEV distribution can be parameterized using harmonic functions. To avoid a possible over-parameterization, an automatic selection model, based on the Akaike Information Criterion, is carried out. Results show that the non-stationary behavior of monthly maxima significant wave height is adequately modeled, drastically increasing the significance of the parameters involved and reducing the uncertainty in the return level estimation. The model provides new information to analyze the seasonal behavior of wave height extremes affecting different natural coastal processes.

75

76 **1. INTRODUCTION**

77

78 Recent advances in the extreme value theory [see Coles, 2001 and Katz et al.,
79 2002 as general references] have appeared in the state-of-the-art allowing a better
80 description of the natural climate variability of extreme events of geophysical variables.
81 The modelling of the seasonality of extreme events can improve our knowledge on
82 some important natural coastal processes such as: the seasonal distribution of benthic
83 organisms in wave-swept environments; the seasonal variability of flow and particle
84 distribution in nearshore seagrass meadows; the influence of wave-exposure on the
85 growth-erosion rates and dislodgement of kelp in the surf zone or the seasonality of the
86 sediment transport rate. The analysis of these processes may require an estimation of a
87 given return-period level conditioned to a given season or month. Moreover, the
88 determination of the return levels of extreme significant wave height, H_s , is vital for
89 other purposes such as coastal management, including the analysis of coastal flooding
90 risk and the design of maritime works. In the latter case, the definition of working time
91 windows during the construction phase or the evaluation of the harbour operation time
92 frames after construction during the winter season requires considering the seasonality
93 or monthly characteristics in the estimation of the return values.

94

95 The calculation of extreme quantiles is often applied to statistical models which
96 use annual maximum data. Due to the scarcity of this type of extreme values, some
97 alternatives are proposed, such as the r -largest maxima method [*Guedes Soares and*
98 *Scotto*, 2004] or the peak over threshold (POT) approach [*Goda*, 2000]. Another
99 possibility is to fit a distribution using monthly maxima [f.i. *Panchang and Li*, 2006]. In

100 general, these methods assume a homogeneous distribution for the extreme population
101 data within a year. However, the hypothesis of homogeneity is not adequately satisfied,
102 since the effects of seasonality are evident [Holthuijsen, 2007]. To illustrate the
103 situation, Figure 1 shows the boxplots for monthly maxima series for five buoys of
104 Puertos del Estado network (see locations in Figure 2). To facilitate the visualization of
105 the extreme events, the winter season has been placed in the center of all Figures. An
106 important modulation in the mean values as well as in the variability of the data is
107 detected.

108

109 In an attempt to model the seasonal behavior of the maximum significant wave
110 height within a year, *Carter and Challenor* [1981] proposed a month-to-month
111 distribution, assuming that data are identically distributed within a given month and
112 analyzing them separately. Subsequently, an annual distribution is obtained by
113 combining the monthly distributions. A similar analysis is performed by *Morton et al.*
114 [1997], applying a seasonal POT model to wind and significant wave height data.

115

116 Basically, all the aforementioned methods require the random variable to be
117 independent and identically distributed (IID) in the block of adopted time (year, season
118 or month). The latter hypothesis can be relaxed to incorporate smooth time variations of
119 the random variable. Examples of this approach applied to different geophysical
120 variables can be found in *Coles* [2001], *Katz et al* [2002] or *Mendez et al.* [2007].
121 Recently, *Mendez et al.* [2006] developed a time-dependent POT model for extreme
122 significant wave height which considers the parameters of the distribution to be
123 functions of time (harmonics within a year, exponential long-term trend, El Niño
124 covariate, etcetera). However, that work focuses on the definition of the higher extreme

125 events of the year (values exceeding a given threshold) and disregards the extreme
126 events in the summer season, therefore being unable to model the entire variability
127 within a year. The object of this article is to develop a time-dependent model based on
128 the GEV distribution, that accounts for seasonality using independent monthly maxima
129 events z_i observed at instants t_i , thus considering 12 maximum values per year. The non-
130 stationary behavior of extreme significant wave height is parameterized using functions
131 of time (harmonic functions) for the parameters of the distribution. The model is
132 applied to five scalar buoys along the Spanish coast (see details in Table 1 and Figure
133 2). Through this approach, the drastic reduction of the uncertainty in the estimation of
134 time-dependent (monthly) quantiles and the improvement in the estimation of annual
135 return values will be shown.

136

137 The paper is organized as follows. Section 2 provides a brief description of the
138 time-dependent generalized extreme value distribution and the parameter estimation
139 method. Section 3 describes the regression model adopted. Next, an automatic model
140 selection procedure is performed and explained in Section 4. The application of the
141 model for the determination of the time-dependent quantiles and the annual quantiles is
142 shown in Section 5. Finally, some conclusions are given in Section 6.

143

144

145 **2. THE TIME-DEPENDENT GEV DISTRIBUTION**

146

147 The monthly maximum method uses time series of block maxima for successive
148 months, $\{Z_t = \max(H_{t1}, \dots, H_{tN})\}$, which are called monthly maxima series (MMS),
149 where the H_{ti} 's, for $i = 1, \dots, N$, are the N values of significant wave height sampled in a

150 given month t and $t = 1, \dots, n$. A critical aspect with discontinuous time series (the buoys
151 records present gaps) is the consideration of a minimum number of data per unit time to
152 define the maxima values. This fact affects the stability of the parameter estimates for
153 the extreme value distribution. After some tests, we adopt the criterion to reject a
154 monthly maximum event if the percentage of gaps for that given month amount over
155 40% [Mendez *et al.*, 2007].

156

157 Considering the apparent temporal dependence within MMS due to seasonal
158 effects, a way to work with MMS is to fit individually the maximum values of each
159 month into a probability distribution and combine the monthly distributions to obtain an
160 annual distribution [Carter and Challenor, 1981]. This implies to fit twelve models,
161 thus obtaining 36 parameters (using, for example, the GEV distribution). This amount
162 of parameters introduces a large uncertainty in the model, diminishing the validity of
163 the results.

164

165 Another possibility to account for this temporal dependence is to use an extension
166 of the standard models of extreme value theory for non-stationary variables [chapter 6,
167 Coles, 2001]). Monthly maxima of successive months are assumed to be independent
168 random variables, but the hypothesis of homogeneity through consecutive months is not
169 needed (because they are not presumed to be identically distributed). We assume that
170 the monthly maximum Z_t of the significant wave heights observed in month t follows a
171 GEV distribution with time-dependent location parameter $\mu(t) > 0$, scale parameter
172 $\psi(t) > 0$, and shape parameter $\xi(t)$. The cumulative distribution function (CDF) of Z_t
173 is then given by

174

$$F_i(z) = \begin{cases} \exp \left\{ - \left[1 + \xi(t) \left(\frac{z - \mu(t)}{\psi(t)} \right) \right]_+^{-1/\xi(t)} \right\} & \xi(t) \neq 0 \\ \exp \left\{ - \exp \left[- \left(\frac{z - \mu(t)}{\psi(t)} \right) \right] \right\} & \xi(t) = 0 \end{cases},$$

(1)

where $[a]_+ = \max[a, 0]$.

The GEV distribution includes three distribution families corresponding to the different form of the tail behavior: Gumbel family in the case of null shape parameter, with a light tail decaying exponentially; Fréchet distribution with $\xi > 0$ and a heavy tail decaying polinomially and Weibull family with $\xi < 0$ and a bounded tail (note that this Weibull for maxima distribution differs from the commonly used Weibull for minima distribution adopted in the POT method for some engineering applications [Goda, 2000]). The probability density function (PDF) of Z_i is obtained by differentiating (1) with respect to z , so that,

$$f_i(z) = \begin{cases} \frac{1}{\psi(t)} \left[1 + \xi(t) \left(\frac{z - \mu(t)}{\psi(t)} \right) \right]_+^{-(1+1/\xi(t))} \exp \left\{ - \left[1 + \xi(t) \left(\frac{z - \mu(t)}{\psi(t)} \right) \right]_+^{-1/\xi(t)} \right\}, & \xi(t) \neq 0 \\ \frac{1}{\psi(t)} \exp \left(- \frac{z - \mu(t)}{\psi(t)} \right) \exp \left[- \exp \left(- \frac{z - \mu(t)}{\psi(t)} \right) \right], & \xi(t) = 0 \end{cases},$$

(2)

For notational purposes, the time-dependent GEV pdf of Equation (2) will be expressed using the following identity:

$$f_i(z) \equiv f_i(z; \theta),$$

(3)

where θ encompasses the three parameters $\mu(t)$, $\psi(t)$ and $\xi(t)$ as indicated later.

195

196 In Section 3, a representation of $\mu(t)$, $\psi(t)$ and $\xi(t)$ by means of harmonic functions
197 (annual cycle, semiannual cycle, etc) will be used. For illustration, Figure 3 shows the
198 time-dependent PDF of equation (2) for the best model found for the Gijon buoy, which
199 uses $\mu(t) = 3.11 + 1.14 \cos(2\pi t) + 0.15 \sin(2\pi t)$ for the location parameter,
200 $\psi(t) = 0.79 + 0.31 \cos(2\pi t) + 0.07 \sin(2\pi t)$ for the scale parameter and $\xi(t) = -0.12$ for
201 the shape parameter. Time t is in years, with origin $t = 0$ at the beginning of the year,
202 and the location and scale parameters are in meters. Note how the seasonality affects the
203 shape of the GEV probability density function, which takes its maximum value for
204 small wave heights in summer ($t = 0.5$ and 1.5 years) but for large wave heights in
205 winter ($t = 0, 1$ and 2 years).

206

207

208 **3. REGRESSION MODEL**

209

210 After a visual inspection of the box-plots of Figure 1, it seems reasonable to allow for
211 seasonality in the model considering harmonic functions within a year. In order to
212 further support this evidence, we examine graphically the variability within a year of the
213 location, scale and shape parameters of the stationary GEV distribution fitted for every
214 month individually. The maximum likelihood estimates (MLEs) $\hat{\mu}$, $\hat{\psi}$ and $\hat{\xi}$ of these
215 parameters over a year (from July to June) for La Coruña buoy are shown in Figure 4.
216 The location parameter shows a single peak, possibly due to the highest extreme events
217 in December-January. The scale parameter is also modulated along a year with a
218 maximum value in the winter season. The results for the shape parameter are not so
219 evident due to the uncertainty in the estimation of this parameter with only one

220 observation per year for every month. Figure 4 also shows the regression fit for the first
221 two harmonics. The good quality of the fit suggests the use of harmonic functions
222 within a year to approximate the seasonal behavior. Mathematically, this model can be
223 expressed as

$$\mu(t) = \beta_0 + \sum_{i=1}^{P_\mu} [\beta_{2i-1} \cos(2i\pi t) + \beta_{2i} \sin(2i\pi t)] \quad (4)$$

$$\psi(t) = \alpha_0 + \sum_{i=1}^{P_\psi} [\alpha_{2i-1} \cos(2i\pi t) + \alpha_{2i} \sin(2i\pi t)] \quad (5)$$

228 provided $\psi(t) > 0$, and

$$\xi(t) = \gamma_0 + \sum_{i=1}^{P_\xi} [\gamma_{2i-1} \cos(2i\pi t) + \gamma_{2i} \sin(2i\pi t)] \quad (6)$$

231
232 where β_0 , α_0 and γ_0 are mean values; β_i , α_i and γ_i ($i > 0$) are the amplitudes of the
233 harmonics; P_μ , P_ψ , and P_ξ are the number of sinusoidal harmonics in a year; and t is
234 given in years.

235
236 The parameters of a possible model (see the example of Figure 3 applied to Gijon buoy)
237 can be packed into the vector $\theta = (\beta_0, \beta_1, \beta_2, \alpha_0, \alpha_1, \alpha_2, \gamma_0)$. In this particular case, the
238 fitted model contains annual cycles for the location and scale parameters,
239 $\mu(t) = \beta_0 + \beta_1 \cos(2\pi t) + \beta_2 \sin(2\pi t)$ and $\psi(t) = \alpha_0 + \alpha_1 \cos(2\pi t) + \alpha_2 \sin(2\pi t)$, and a
240 constant value for the shape parameter $\xi(t) = \gamma_0$. The number of significantly non-null
241 regression parameters is therefore $p = 7$.

242
243 For any of the candidate models, represented by its vector parameter θ , and for m
244 observations of monthly maxima Z_{t_i} occurring at instants t_i , we estimate the model
245 parameters $\hat{\theta}$ using the method of maximum likelihood. Approximate standard errors,
246 $se(\hat{\theta})$, for the estimators, and 95% confidence intervals,
247 $(\hat{\theta}_i - 1.96se(\hat{\theta}_i), \hat{\theta}_i + 1.96se(\hat{\theta}_i))$, for the regression parameters, are obtained using
248 standard likelihood theory (see details in Appendix A).

249

250

251 **4. MODEL SELECTION**

252

253 **4.1. Codification**

254 In this work, we consider the largest parameterization with two sinusoidal harmonics
255 ($P_\mu = 2$, $P_\psi = 2$ and $P_\xi = 2$). Moving from the simplest model $\theta^1 = (\beta_0, \alpha_0)$ (that is, a
256 homogeneous Gumbel distribution) to the most complex one
257 $\theta^b = (\beta_0, \beta_1, \beta_2, \beta_3, \beta_4, \alpha_0, \alpha_1, \alpha_2, \alpha_3, \alpha_4, \gamma_0, \gamma_1, \gamma_2, \gamma_3, \gamma_4)$, we have a large variety of
258 models to choose from, many of them having different degrees of freedom. Following
259 the genetic algorithms nomenclature [Goldberg, 1989], we adopt a binary codification
260 to represent each model, according to the involved factors. Therefore, every model is
261 encoded using a binary chromosome, $c = [g_1 g_2 \cdot g_3 g_4 \cdot g_5 \cdot g_6 g_7]$, where g_i are binary genes
262 which represent given factors. Each gene g_i has two possible values, $g_i = 1$ if the i th
263 factor is switched on and $g_i = 0$ if it is switched off. Gene g_1 represents the annual
264 cycle (β_1, β_2) for the location parameter, $g_2 (\beta_3, \beta_4)$ the semiannual cycle for the

265 location parameter, $g_3(\alpha_1, \alpha_2)$ the annual cycle for the scale parameter, $g_4(\alpha_3, \alpha_4)$ the
266 semiannual cycle for the scale parameter, g_5 is a gene that includes a constant non-zero
267 shape parameter (γ_0), $g_6(\gamma_1, \gamma_2)$ allow for the annual cycle for the shape parameter
268 and $g_7(\gamma_3, \gamma_4)$ the semiannual cycle for the shape parameter.

269

270 For example, the simplest model $\theta^1 = (\beta_0, \alpha_0)$ has a binary chromosome
271 $c^1 = [00.00.0.00]$ and the saturated model θ^b has a binary
272 chromosome $c^b = [11.11.1.11]$. The model shown previously for Gijon buoy has the
273 vector parameter $\theta = (\beta_0, \beta_1, \beta_2, \alpha_0, \alpha_1, \alpha_2, \gamma_0)$, so that its binary chromosome is
274 $c = [10.10.1.00]$.

275

276 **4.2.Fitness criteria**

277

278 The quality of a particular model i , with a binary chromosome c^i (and
279 consequently a vector parameter θ^i) is assessed by using a penalized function based on
280 the Akaike information criterion [Akaike, 1973],

281

$$282 \quad \text{AIC}_i = -2\ell(\hat{\theta}^i | t_j, z_j) + 2p_i, \quad (7)$$

283

284 where p_i is the number of parameters, and $\ell(\hat{\theta}^i | t_j, z_j)$ is the maximum of the log-
285 likelihood resulting from model “ i ” for the sample $\{t_j, z_j\}$. Equation (7) establishes a
286 compromise between obtaining a good fit, which is measured by how small the
287 resulting $-2\ell(\hat{\theta}^i | t_j, z_j)$ term is, and using a simple model, where simpler models use

288 less parameters than complex models. Therefore, the smaller the criterion, the better the
289 model.

290

291 **4.3. Automatic selection**

292

293 For the particular codification proposed in this work, we have $2^7 = 128$ models to
294 select the best one. Instead of naive procedures, such as exploring all the possible
295 models, we use a stepwise algorithm that combines forward selection and backward
296 elimination procedures. In addition to the steps performed in the forward selection
297 algorithm, all non-zero genes are tested backward to see if their contributions are
298 significant after a new gene has been switched on. This may lead to the elimination of
299 an already selected gene if its factor has become superfluous because its effects may be
300 represented by other factor. The criterion to incorporate a given factor is based on the
301 AIC statistic given by Equation (7). Table 2 and Figure 5 show the application of this
302 automatic selection procedure to the data set of the Valencia buoy. In Table 2, we show
303 the binary chromosome, maximum likelihood estimates, log-likelihood function ℓ ,
304 number of parameters p and AIC value. Figure 5 shows the location parameter (solid
305 lines), the scale parameter (dashed lines) and the 20-year return period time-dependent
306 quantile (bold lines). The starting model is $c^1 = [00.00.0.00]$ and the final model after 6
307 steps is $c^6 = [11.11.1.00]$ (two harmonics for the location and scale parameters and a
308 constant non-zero value for the shape parameter).

309

310 For this particular case, the incorporation factor sequence is: (step 2) annual cycle
311 for the scale parameter; (3) annual cycle for the location parameter; (4) semiannual
312 cycle for the scale parameter; (5) semiannual cycle for the location parameter; and (6) a

313 constant non-zero value for the shape parameter. Note how the location and scale
314 parameters as well as the quantile progressively improve the fit. Particularly interesting
315 is the bimodal behavior of monthly maxima in Valencia buoy, suggesting two extreme
316 seasons (Fall and beginning of Spring) throughout the year.

317

318 **4.4. Model diagnostic**

319

320 The model-checking of the best model obtained is evaluated graphically by means
321 of quantile-quantile (QQ) and probability-probability (PP) plots. We standardize the
322 maximum Z_t using

323

$$324 \quad \bar{Z}_t = \frac{1}{\hat{\xi}(t)} \log \left[1 + \hat{\xi}(t) \left(\frac{Z_t - \hat{\mu}(t)}{\hat{\psi}(t)} \right) \right],$$

325 (8)

326 so that \bar{Z}_t would follow a standard Gumbel distribution if the model and parameter
327 values were exactly true. Probability and quantile plots for the sample of computed
328 values \bar{z}_t can be obtained using Eq. (8). If $\bar{z}_{(1)}, \dots, \bar{z}_{(m)}$ are the corresponding sample
329 order statistics, the plotting points (e.g., empirical vs model) for the probability plot are
330 $\{i/(m+1), \exp(-\exp(-\bar{z}_{(i)}))\}$ whilst the plotting points for the quantile plot are
331 $\{-\log(-\log(i/(m+1))), \bar{z}_{(i)}\}$ for $i = 1, \dots, m$. We can see in Figure 6 that, for the Valencia
332 data set and for the best model $c^6 = [11.11.1.00]$, the PP and QQ plots show very good
333 diagnostics, with points close to the diagonal. Similar plots have been obtained for the
334 remaining locations, although they are no shown for space limitations.

335

336

337 5. INFERENCE FOR RETURN LEVELS

338

339 5.1. Time-dependent quantiles

340

341 For non-stationary or time-dependent GEV parameters, the calculation of

342 “effective” design value quantiles can be carried out using

343

$$344 \quad z_q(t, \theta) = z_q(\mu(t), \psi(t), \xi(t)) = \begin{cases} \mu(t) - \frac{\psi(t)}{\xi(t)} \left[1 - \{-\log(1-q)\}^{-\xi(t)} \right] & \xi(t) \neq 0 \\ \mu(t) - \psi(t) \log\{-\log(1-q)\} & \xi(t) = 0 \end{cases},$$

345 (9)

346

347 where probability q is given by $F_t(z) = 1 - q$ and the quantile estimate $\hat{z}_q(t, \hat{\theta})$ is the

348 time-dependent return level associated with the return period $1/q$. Therefore, the

349 quantity varies depending on the time of the year [Méndez *et al.*, 2007]. Confidence

350 intervals can be obtained by the delta method [Rice, 1994], assuming approximate

351 normality for the maximum likelihood estimators.

352

353 Figure 7 shows, for the Bilbao data set, the comparison between the stationary

354 model applied month-to-month and the best time-dependent model, both with 20-year

355 return period quantiles and 95% confidence intervals. Note how the confidence intervals

356 are reduced with the time-dependent model and how the point estimates are more

357 consistent with each other. The month-to-month approach may lead to unreliable

358 estimates, as seen in the months of January and February. This is due to the fact that,

359 instead of using a sample of 14 – 19 maximum values for the estimation month-to-

360 month, we are using a sample of 190 values when modeling the seasonal behavior
361 within a year. This results in a better explanation of data variability, a reduction in the
362 uncertainty of the quantile estimates and a better estimation for return values in any
363 month or season, as this methodology uses all the surrounding information throughout
364 the year.

365

366 We have applied the methodology to the five buoys, obtaining for each particular
367 case the model that best fits the data ($c^{BI} = c^{GI} = [10.10.1.00]$, $c^{CO} = [10.11.1.00]$,
368 $c^{CA} = [11.11.0.10]$ and $c^{VA} = [11.11.1.00]$). Numerical values of the maximum
369 likelihood estimates of the best model for each buoy are shown in Table 3. Figure 8
370 shows, for each selected model, the location parameter (solid line), the time-dependent
371 20-year return period quantile (bold-solid line) and the 95% confidence interval (dashed
372 lines). Observed values of monthly maxima significant wave heights are indicated by
373 crosses. One can see that the fit is remarkably good for all the cases, each of them
374 presenting a different parameterization. To further assess the goodness of fit we have
375 evaluated the proportions of data for the studied MMS falling below $\mu(t)$ or $H_{20}(t)$;
376 these proportions show an averaged absolute deviation of 0.0136 with regard to the
377 theoretical value of 0.37 for $\mu(t)$ and 0.0046 with regard to the theoretical value of 0.95
378 for $H_{20}(t)$.

379

380 The results obtained for Bilbao and Gijon present an annual cycle for the location
381 and the scale parameter and a negative value for the scale parameter (upper bounded
382 tail), clearly pointing at the winter season (from November to March). In the case of La
383 Coruña, a semiannual cycle in the scale parameter is also significant. The western
384 location of La Coruña buoy causes a wider winter season than that seen in the Gijon and

385 Bilbao buoys, that being more exposed to west winter cyclones. The data set from Cadiz
386 is the only one presenting a significative annual cycle for the shape parameter; resulting
387 in a short tailed behavior in the summer season, due to local storms, and a long tailed
388 one in the winter season (November to February), due to long-fetched storms. The
389 modulation of seasonality showed in the Valencia buoy is a well-known pattern along
390 the Spanish Mediterranean coast. It presents two peaks of maxima significant wave
391 heights, one resulting from ‘*gota fria*’ phenomenon in the fall season (warming of
392 Mediterranean Sea together with cyclones) and another in the spring season. The
393 knowledge of the seasonal distribution of the location, scale and shape parameters
394 allows estimating quantitatively the intrannual variability of extreme wave climate. The
395 location parameter (which coincides with the mode of the distribution) varies in a range
396 of about two meters in the Atlantic buoys (for the case of La Coruña is almost three
397 meters), whereas the range of Valencia buoy, in the Mediterranean Sea, is less than half
398 meter. The scale parameter shows the highest range (almost one meter) in Cadiz buoy
399 and is greatly influenced by the semiannual cycle in La Coruña and Valencia buoys.

400

401 **5.2. Annual quantiles**

402

403 The calculation of extreme significant wave height return values for a given period
404 (year, season or month) requires a more complex approach. With time-dependent GEV
405 parameters, determinating a return period involves combining probabilities that differ
406 depending on the day within a year (see chapter 7 in *Coles*, [2001]). A similar procedure
407 for mixed populations was proposed by *Carter and Challenor* [1981] using twelve
408 distributions for monthly maxima, and by *Morton et al.* [1997] using four seasonal POT
409 distributions.

410

411 In particular, the annual quantile return level $\bar{z}_q[t_1, t_2]$ corresponding to a given
412 probability $1 - q$ and an interval $[t_1, t_2]$, equal or larger than one month, can be obtained
413 by iteratively solving the equation:

$$1 - q = \exp \left\{ -k_m \int_{t_1}^{t_2} \left[1 + \xi(t) \left(\frac{\bar{z}_q[t_1, t_2] - \mu(t)}{\psi(t)} \right) \right]_{+}^{-1/\xi(t)} dt \right\},$$

(10)

416 where $1/k_m$ is the length of the block maxima, that is, one month ($1/k_m = 1/12$ year).

417

418 Figure 9 shows the monthly and annual return level plot for Gijón's best model. This
419 figure is obtained by successively taking the interval $[t_1, t_2]$ in equation (10) equal to
420 each month from January to December and subsequently taking $[t_1, t_2]$ equal to the
421 whole year. The figure shows, for example, that significant wave height attains a value
422 of 8 meters once every 31 years, but only once every 77 Januaries, once every 105
423 Decembers, and so on. A bounded tail behavior (Weibull family) is detected. Note that
424 the winter months (December, January and February) present the highest monthly
425 quantiles whereas the summer months show the lowest monthly quantiles.

426

427 Although not required by our method, comparison with alternative formulations may be
428 facilitated by expressing equation (10) in terms of the rescaled annual maxima GEV
429 parameters $\mu^*(t)$, $\psi^*(t)$, $\xi^*(t)$ [Dixon and Tawn, 1994]. Thus it may be easily verified
430 that the right hand side of equation (10) is exactly equal to

431

$$\exp \left\{ -k_y \int_{t_1}^{t_2} \left[1 + \xi^*(t) \left(\frac{\bar{z}_q[t_1, t_2] - \mu^*(t)}{\psi^*(t)} \right) \right]_+^{-1/\xi^*(t)} dt \right\},$$

(11)

where $1/k_y = 1$ year, $\mu^*(t) = \mu(t) + \frac{\psi(t)}{\xi(t)} \left[\left(\frac{k_m}{k_y} \right)^{\xi(t)} - 1 \right]$, $\psi^*(t) = \psi(t) \cdot \left(\frac{k_m}{k_y} \right)^{\xi(t)}$ and

$\xi^*(t) = \xi(t)$.

6. CONCLUSIONS

A statistical model to analyze the seasonality of monthly maxima significant wave heights is presented. The model is based on the time-dependent generalized extreme value distribution for independent monthly maxima series of significant wave heights. Non-stationarity is introduced in the model using cosine functions that represent the annual and semiannual cycles. These factors are included in the location, scale and shape parameters of the probability distribution of extreme significant wave height. The inclusion of seasonal variabilities substantially reduces the residuals of the fitted model. To avoid over-parameterization, an automatic model selection procedure based on the Akaike Information Criterion is carried out.

The developed time-dependent methodology provides more reliable results than the stationary model of individually month-to-month analysis. For a particular month, we are using not only the maximum values from this month but also the information of the neighbour months, thus including the natural climate variability. Therefore, we

455 believe that the large discrepancy in the month-to-month method is due to unduly
456 sampling variation.

457

458 The model is applied to five buoys of Puertos del Estado network (Bilbao, Gijon,
459 La Coruña, Cadiz and Valencia) showing seasonality characteristics of the wave climate
460 of these particular sites. Obtained results show that the model provides a tool for
461 quantitatively examining the long-term seasonal distribution, using monthly maxima of
462 significant wave heights. The methodology provides time-dependent and annual return-
463 period values and their confidence intervals. The information obtained in this study can
464 be useful to better understand several issues governed by ocean waves such as
465 distribution of organisms in wave-swept environments, coastal management or the
466 design of maritime works.

467

468 The applicability of our methods to various Spanish buoys with different wave climate
469 conditions and the flexibility of the time-dependent GEV distribution (that allows
470 modeling the seasonality and varied upper tail behaviors), reinforces the possibility of
471 using the same methods to analyze other geophysical variables such as sea surface
472 temperature, wind velocity or sea level.

473

474 We believe that the model provides a new way to gain further insights in our
475 knowledge of climate variability of extreme events. We have analyzed just seasonal
476 processes but the methodology should be able to deal with different time scales, such as
477 long-term trends or interannual variability (North Atlantic Oscillation, Southern
478 Oscillation, etcetera).

479

480

481 **APPENDIX A. Parameter estimation**

482

483 We use the method of maximum likelihood to estimate the model parameters. The
 484 location, scale and shape parameters $\mu(t)$, $\psi(t)$ and $\xi(t)$ are expressed in terms of
 485 harmonic functions whose amplitudes are regression parameters that must be estimated
 486 [Coles, 2001]. The complete vector of p regression parameters is denoted by θ . The
 487 likelihood function of the parameters for any given sample $\{(t_1, z_1), \dots, (t_m, z_m)\}$ of the
 488 periods t_i at which the maxima z_i are attained, is provided by

489

490

$$L(\theta | t_i, z_i) = \prod_{i=1}^m f_i(z_i, \theta) = \prod_{i=1}^m f_i(z_i; \mu(t_i), \psi(t_i), \xi(t_i)) \quad (12)$$

493

494 where $f_i(z; \mu(t), \psi(t), \xi(t))$ is the time-dependent GEV pdf given by Equation (2). The
 495 log-likelihood function is

$$\begin{aligned} \ell(\theta | t_i, z_i) = & - \sum_{i=1}^m \left\{ \log \psi(t_i) + (1 + 1/\xi(t_i)) \log \left[1 + \xi(t_i) \left(\frac{z_i - \mu(t_i)}{\psi(t_i)} \right) \right] \right\}_+ \\ & + \left[1 + \xi(t_i) \left(\frac{z_i - \mu(t_i)}{\psi(t_i)} \right) \right]_+^{-1/\xi(t_i)} \end{aligned} \quad (13)$$

498 provided that $\psi(t_i) > 0$ for $i = 1, \dots, m$. For every value of $\xi(t_i)$ that equals zero, the
 499 appropriate limiting form must be used, replacing the GEV by the Gumbel (equation (1)
 500 for $\xi = 0$) log-likelihood function,

$$\ell(\theta | t_j, z_j) = -\log \psi(t_j) - \frac{z_j - \mu(t_j)}{\psi(t_j)} - \exp\left[-\frac{z_j - \mu(t_j)}{\psi(t_j)}\right]. \quad (14)$$

Maximization of (13) and/or (14) yields to $\ell(\hat{\theta} | t_j, z_j)$ and the maximum likelihood estimate of θ , denoted by $\hat{\theta}$. A global optimization procedure, namely the shuffled complex evolution (SCE) algorithm [Duan *et al.* 1992] is used to compute the parameter estimates.

An advantage of adopting maximum likelihood for parameter estimation is that a widely applicable approximation for standard errors and confidence intervals is available based on asymptotic properties of maximum likelihood estimators. Solving log-likelihood equations, we can evaluate the observed information matrix at $\theta = \hat{\theta}$. Assessing the inverse of this matrix and then the square roots of the diagonal entries, we obtain approximate values for the asymptotic standard errors of the parameters estimates, abbreviated $se(\hat{\theta}_i)$. Confidence intervals for θ_i can be obtained in the form $[\hat{\theta}_i - z_\alpha se(\hat{\theta}_i), \hat{\theta}_i + z_\alpha se(\hat{\theta}_i)]$, where $se(\hat{\theta}_i)$ is the standard error of the ML estimator $\hat{\theta}_i$ and $z_{0.95} = 1.96$ gives approximate confidence intervals of 95%.

524

525 **Acknowledgements**

526 The authors would like to thank “Puertos del Estado” for providing the information
527 from the instrumental observation networks. The work was partially funded by projects
528 ENE2004-08172 and CGL2005-05365/CLI from the Spanish Ministry of Educación y
529 Ciencia. Melisa Menéndez and Fernando J. Méndez are indebted to the Spanish
530 Ministry of Educación y Ciencia for funding them through the FPI and “Ramón y
531 Cajal” program, respectively. Alberto Luceño acknowledges the support of the Spanish
532 Dirección General de Investigación under Grant MTM2005-00287.

533

534

535 **REFERENCES**

536

537 Akaike, H. (1973) Information theory and an extension of the maximum likelihood
538 principle, in: B.N. Petrov and F. Csáki, eds. Proc. 2nd Internat. Symp. on Information
539 Theory (Akadémia Kiadó, Budapest) pp. 267–281.

540

541 Carter, D. J. T., and P. G. Challenor (1981) Estimating return values of environmental
542 variables. *Quart. J. Roy. Meteor. Soc.*, 107, 259-266.

543

544 Coles, S. G. (2001) *An introduction to statistical modelling of extreme values*. London:
545 Springer, 208 pp.

546

547 Dixon, M. J. and J. A. Tawn (1994) Extreme sea-levels at the U.K. A class-sites: site by
548 site analysis. Proudman Oceanographic Laboratory Internal Document 65, 228 pp.

549

- 550 Duan, Q., S. Sorooshian, and V. Gupta (1992) Effective and efficient global
551 optimization for conceptual rainfall-runoff models. *Water Resour. Res.*, 28, 1015-1031.
552
- 553 Goda, Y. (2000) *Random seas and design of maritime structures*. Advanced Series on
554 Ocean Engineering , Vol. 15. World Scientific. Ed. P. L.-F. Liu., 443 pp.
555
- 556 Goldberg, D.E. (1989) *Genetic algorithms in search, optimization, and machine*
557 *learning*, Addison-Wesley, Reading, Mass, 372 pp.
558
- 559 Guedes Soares, C., and M. G. Scotto (2004) Application of the r-largest order statistics
560 for long-term predictions of significant wave height. *Coast. Eng.*, 51, 387-394.
561
- 562 Holthuijsen, L.H. (2007) *Waves in Oceanic and Coastal Waters*, Cambridge University
563 Press. 404 pp.
564
- 565 Katz, R. W., M. B. Parlange, and P. Naveau (2002) Statistics of extremes in hydrology.
566 *Adv. in Water Resour.*, 25, 1287-1304.
567
- 568 Méndez, F.J., Menéndez, M., Luceño, A., Losada, I.J. (2006) Estimation of the long-
569 term variability of extreme significant wave height using a time-dependent POT model,
570 *Journal of Geophysical Research*, Vol. 111, C07024, doi: 10.1029/2005JC003344.
571
- 572 Méndez, F.J., Menéndez, M., Luceño, A., Losada, I.J. (2007) Analyzing monthly
573 extreme sea levels with a time-dependent GEV model, *Journal of Atmospheric and*
574 *Oceanic Technology*, 24, 894-911, doi: 10.1175/JTECH2009.1.
575

576 Morton, I.D., J. Bowers, and G. Mould (1997) Estimating return period wave heights
577 and wind speeds using a seasonal point process model, *Coastal Eng.*, 31, 305-326.

578

579 Panchang, V.G. and D. Li (2006) Large waves in the Gulf of Mexico caused by
580 Hurricane Ivan, *Bulletin of the American Meteorological Society*, 481-489.

581

582 Rice, J. (1994) *Mathematical Statistics and Data Analysis*, 2nd ed., Duxbury, Pacific
583 Grove, Calif, 651pp.

584

585

586

587

588

589

590

591

592

593

594

595

596

597

598

599

600

601

602

	Water depth (m)	Period of measurement	Number of monthly maxima
Bilbao (BI)	50	1985-2003	190
Gijón (GI)	23	1984-2002	199
Coruña (CO)	50	1984-2003	179
Cádiz (CA)	22	1984-2002	174
Valencia (VA)	20	1985-2003	170

603

604

605 Table 1. Descriptive issues of the buoys used in the analysis

606

607

608

609

610

611

612
 613
 614

Step	1	2	3	4	5	6
Chromosome	[00.00.0.00]	[00.10.0.00]	[10.10.0.00]	[10.11.0.00]	[11.11.0.00]	[11.11.1.00]
β_0 (cm)	157.4 (4.3)	150.8 (3.7)	158.6 (3.4)	156.9 (2.96)	158.6 (4.9)	161.6 (4.9)
β_1 (cm)	-	-	22.8 (4.1)	21.8 (2.9)	18.1 (5.3)	19.0 (5.5)
β_2 (cm)	-	-	0.07 (4.3)	-0.38 (5.4)	1.5 (9.2)	1.2 (6.7)
β_3 (cm)	-	-	-	-	-11.2 (4.1)	-12.1 (5.7)
β_4 (cm)	-	-	-	-	2.8 (7.5)	2.0 (5.9)
α_0 (cm)	53.9 (3.3)	52.6 (1.4)	52.3 (2.2)	51.8 (2.9)	51.6 (3.7)	53.7 (3.7)
α_1 (cm)	-	17.4 (2.6)	23.8 (4.0)	18.4 (3.0)	17.9 (5.9)	18.2 (4.2)
α_2 (cm)	-	3.2 (3.0)	2.7 (3.6)	3.1 (4.8)	3.1 (4.2)	2.6 (4.7)
α_3 (cm)	-	-	-	-8.7 (4.2)	-10.6 (5.2)	-12.4 (4.5)
α_4 (cm)	-	-	-	-3.7 (4.1)	-3.2 (4.3)	-6.0 (4.4)
γ_0	-	-	-	-	-	-0.106 (0.06)
γ_1	-	-	-	-	-	-
γ_2	-	-	-	-	-	-
γ_3	-	-	-	-	-	-
γ_4	-	-	-	-	-	-
ℓ	-948.54	-942.60	-935.18	-932.54	-930.36	-929.21
p	2	4	6	8	10	11
AIC	1901.1	1893.2	1882.4	1881.1	1880.7	1880.4

615
 616
 617
 618
 619
 620
 621

Table 2. Summary of the results for the stepwise evolution of the Valencia buoy: chromosome, maximum likelihood estimates of the parameters with standard errors (in parentheses), maximum of the log-likelihood function (ℓ), number of parameters involved (p) and Akaike Information Criteria statistic (AIC).

622
623
624
625
626
627

Buoy	BI	GI	CO	CA	VA
Chromosome	[10.10.1.00]	[10.10.1.00]	[10.11.1.00]	[11.11.0.10]	[11.11.1.00]
β_0 (cm)	325.3 (6.9)	310.7 (6.6)	409.8 (9.0)	216.8 (6.4)	161.6 (4.8)
β_1 (cm)	99.5 (8.6)	114.2 (8.3)	142.9 (11.1)	94.4 (10.3)	19.0 (5.5)
β_2 (cm)	13.5 (8.1)	15.4 (7.7)	16.4 (12.2)	11.7 (6.6)	1.2 (6.7)
β_3 (cm)	-	-	-	19.6 (5.8)	-12.1 (5.6)
β_4 (cm)	-	-	-	-16.7 (5.3)	2.0 (5.8)
α_0 (cm)	80.8 (4.9)	79.1 (4.6)	105.2 (6.6)	62.4 (4.7)	53.7 (3.6)
α_1 (cm)	29.4 (6.1)	31.4 (6.3)	24.6 (7.9)	59.0 (7.7)	18.2 (4.2)
α_2 (cm)	9.0 (5.6)	6.7 (4.9)	-0.2 (8.9)	0.9 (5.2)	2.6 (4.6)
α_3 (cm)	-	-	-15.5 (8.1)	15.8 (4.7)	-12.4 (4.5)
α_4 (cm)	-	-	-3.7 (9.0)	-9.1 (4.0)	-6.0 (4.4)
γ_0	-0.13 (0.05)	-0.12 (0.05)	-0.14 (0.05)	-	-0.11 (0.06)
γ_1	-	-	-	-0.17 (0.08)	-
γ_2	-	-	-	0.03 (0.07)	-
γ_3	-	-	-	-	-
γ_4	-	-	-	-	-
p	7	7	9	12	11

628
629
630
631
632
633

Table 3. Summary of the final results for the time-dependent model for the studied buoys: final chromosome, maximum likelihood estimates for the location, scale and shape parameters (with standard errors) and number of involved parameters.

634
635
636
637
638

FIGURE CAPTIONS

639 Figure 1. Boxplots for monthly maxima significant wave height in Bilbao, Gijon, La
640 Coruña, Cadiz and Valencia buoys. Trapezoidal boxes have lines at the lower quartile,
641 median and upper quartile values. The whiskers extend to the 1.5 interquartile range or
642 to the range of the data, whichever is shorter, and crosses show unusual values.

643

644 Figure 2. Location of the buoys (BI, GI, CO, CA and VA stands for Bilbao, Gijon, La
645 Coruña, Cadiz and Valencia, respectively)

646

647 Figure 3. Time-dependent GEV probability density function for Gijon with the final
648 parameterization.

649

650 Figure 4. Scatter plots of annual stationary GEV parameter estimates (each for a given
651 month) along a year for La Coruña buoy. Regression fit to one (grey line) and two
652 (black line) harmonics is also plotted.

653

654 Figure 5. Evolution of the stepwise method for Valencia buoy, starting from
655 $c_1 = [00.00.0.00]$ (stationary case) and ending in $c_6 = [11.11.1.00]$ (two harmonics for
656 the location and scale parameters and a constant non-zero value for the shape
657 parameter). Location parameter is indicated in solid lines, scale parameter in dashed
658 lines and 20-year time-dependent return level in bold lines.

659

660 Figure 6. Probability (left) and quantile (right) plots for the best model $c^6 = [11.11.1.00]$
661 for the Valencia data set.

662

663 Figure 7. Comparison between the stationary model applied month-to-month (the
664 midpoint are the 20-year return level and the vertical lines are the 95% confidence
665 interval) and the time-dependent model for Bilbao data set (solid line is the 20-year
666 return period quantile and dashed lines 95% confidence interval).

667

668 Figure 8. 20-year return period quantiles (bold lines) within a year and 95% confidence
669 intervals (dashed lines). The lower lines show the time-dependent location parameter.
670 Observed values of monthly maxima significant wave height indicated by crosses.
671 Results are for the best model for the five buoys.

672

673 Figure 9. Monthly and annual return level plots for Gijon buoy.

674

675

676

677

678

679

680

681

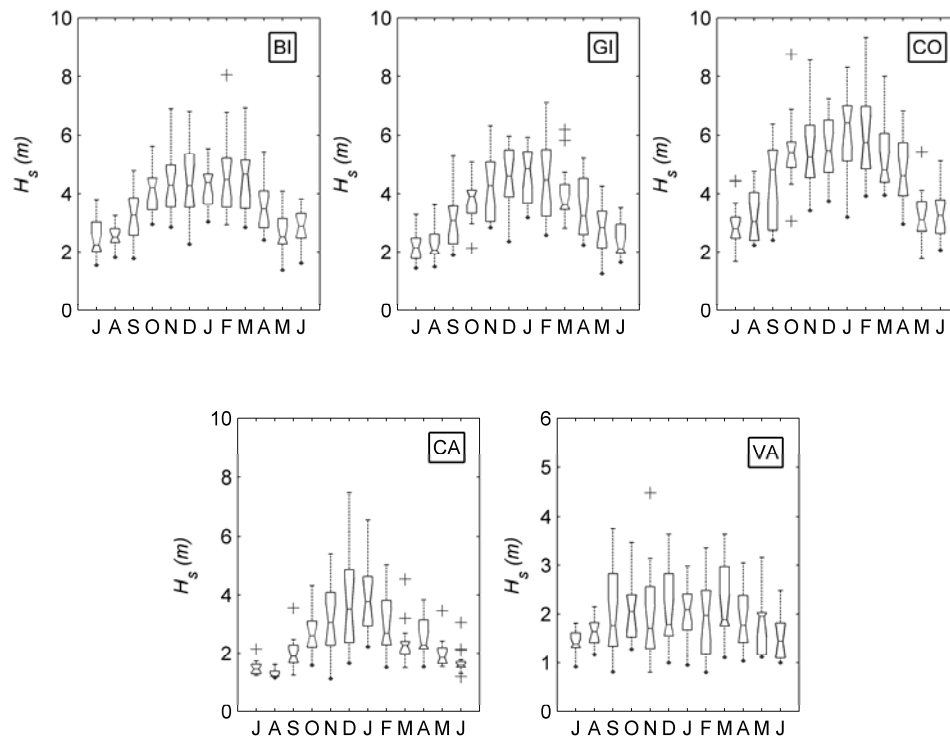
682

683

684

685

686
687
688
689
690



691
692
693
694
695
696
697
698
699

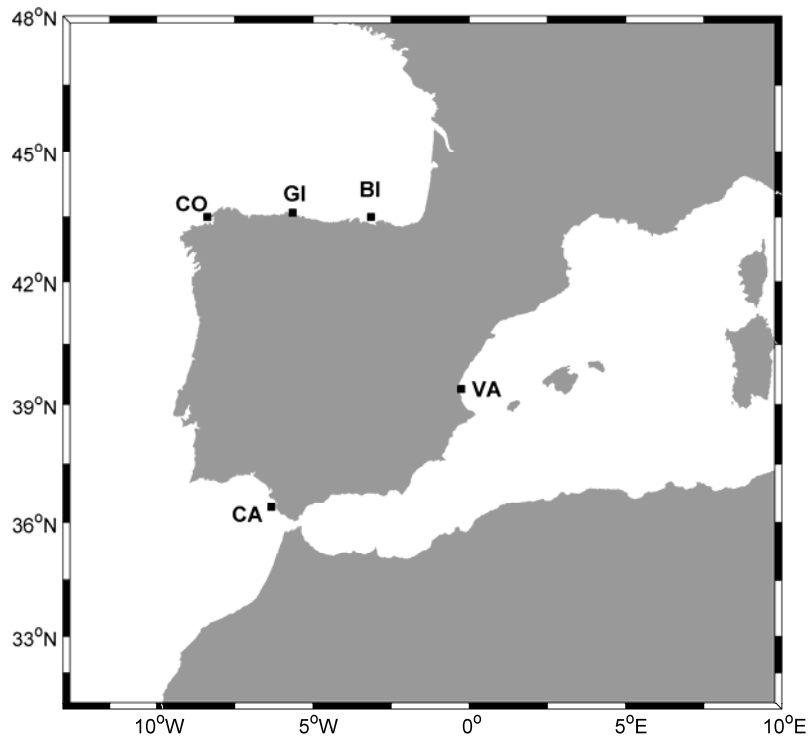
Figure 1. Boxplots for monthly maxima significant wave height in Bilbao, Gijón, La Coruña, Cadiz and Valencia buoys. Trapezoidal boxes have lines at the lower quartile, median and upper quartile values. The whiskers extend to the 1.5 interquartile range or to the range of the data, whichever is shorter, and crosses show unusual values.

700

701

702

703



704

705 Figure 2. Location of the buoys (BI, GI, CO, CA and VA stands for Bilbao, Gijon, La

706 Coruña, Cadiz and Valencia, respectively)

707

708

709

710

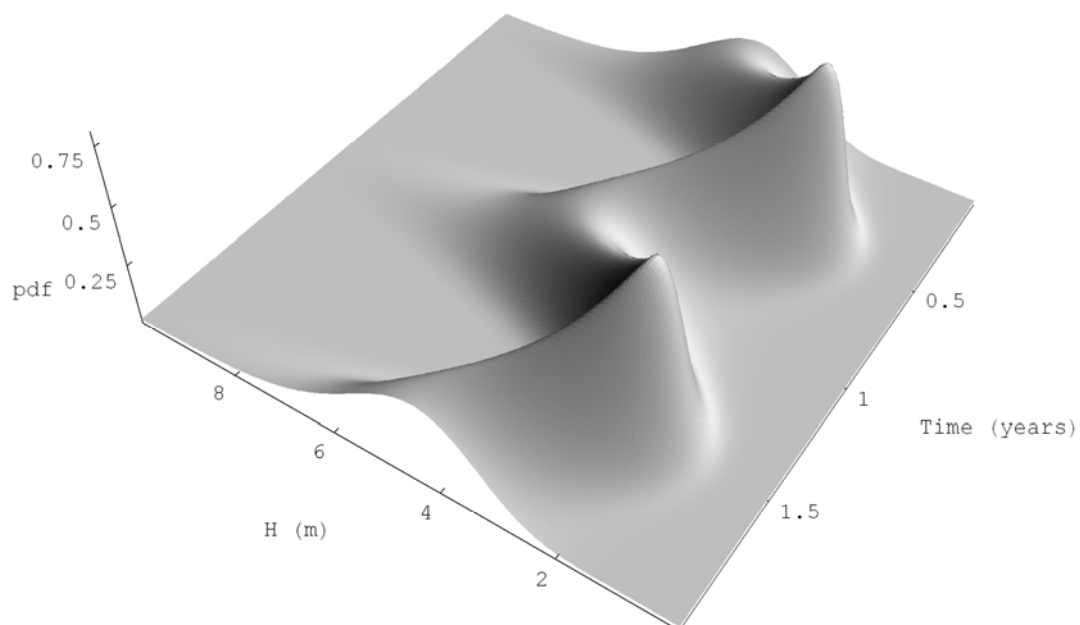
711

712

713

714

715



716

717 Figure 3. Time-dependent GEV probability density function for Gijón with the final
718 parameterization.

719

720

721

722

723

724

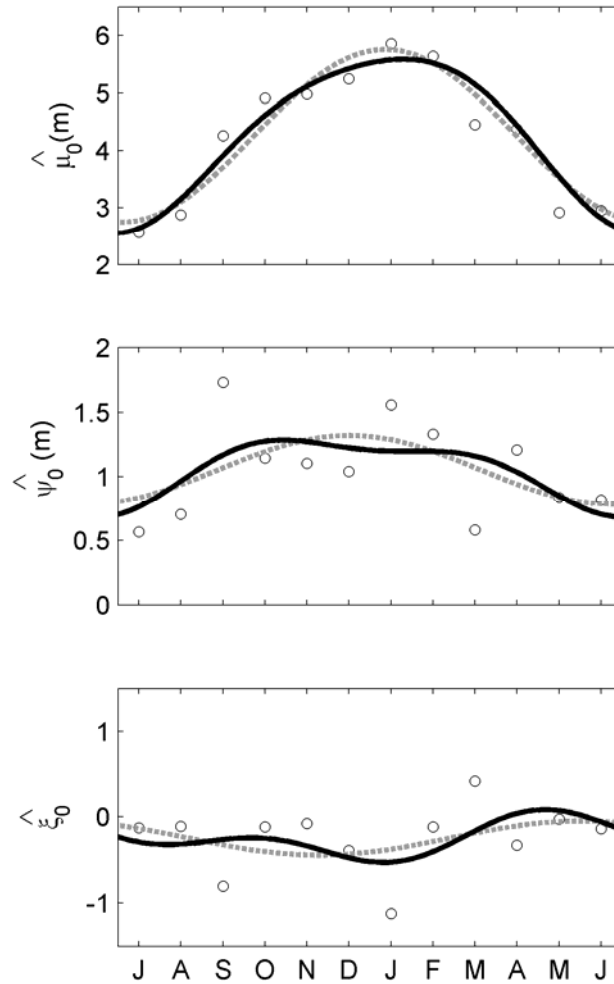
725

726

727

728

729



730

731

732 Figure 4. Scatter plots of annual stationary GEV parameter estimates (each for a given

733 month) along a year for La Coruña buoy. Regression fit to one (grey line) and two

734 (black line) harmonics is also plotted.

735

736

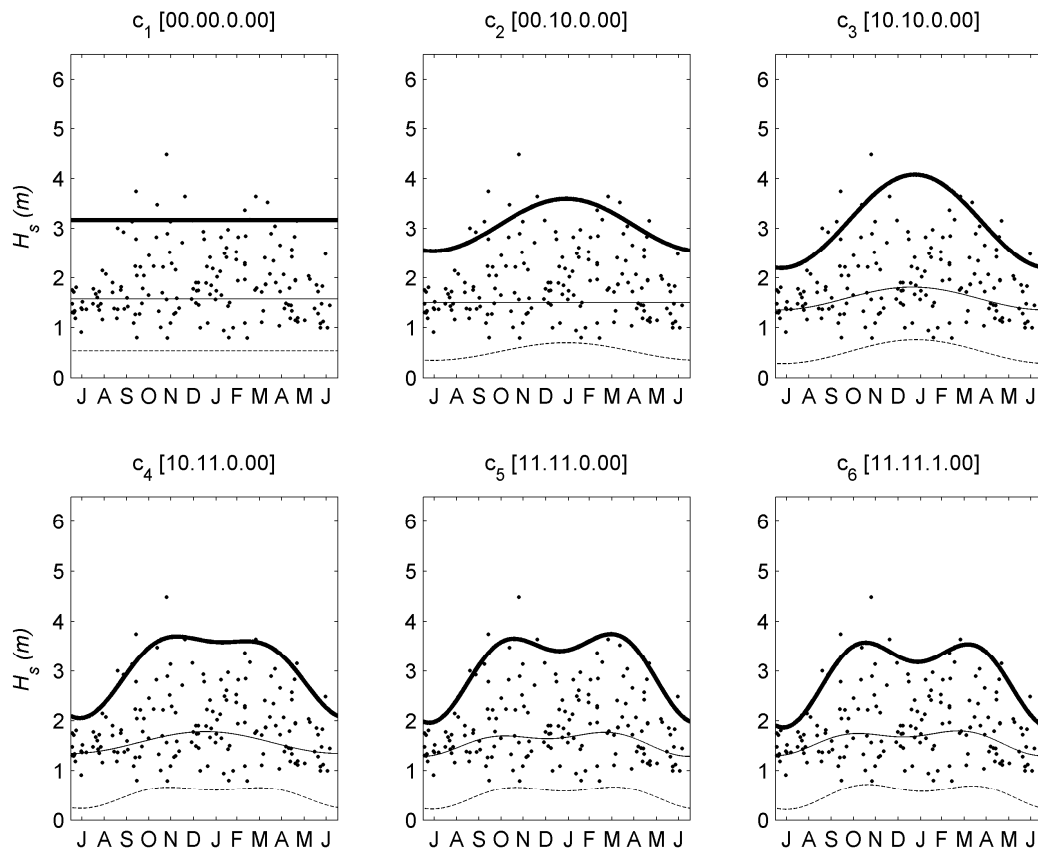
737

738

739

740

741



742

743 Figure 5. Evolution of the stepwise method for Valencia buoy, starting from

744 $c_1 = [00.00.0.00]$ (stationary case) and ending in $c_6 = [11.11.1.00]$ (two harmonics for

745 the location and scale parameters and a constant non-zero value for the shape

746 parameter). Location parameter is indicated in solid lines, scale parameter in dashed

747 lines and 20-year time-dependent return level in bold lines.

748

749

750

751

752

753

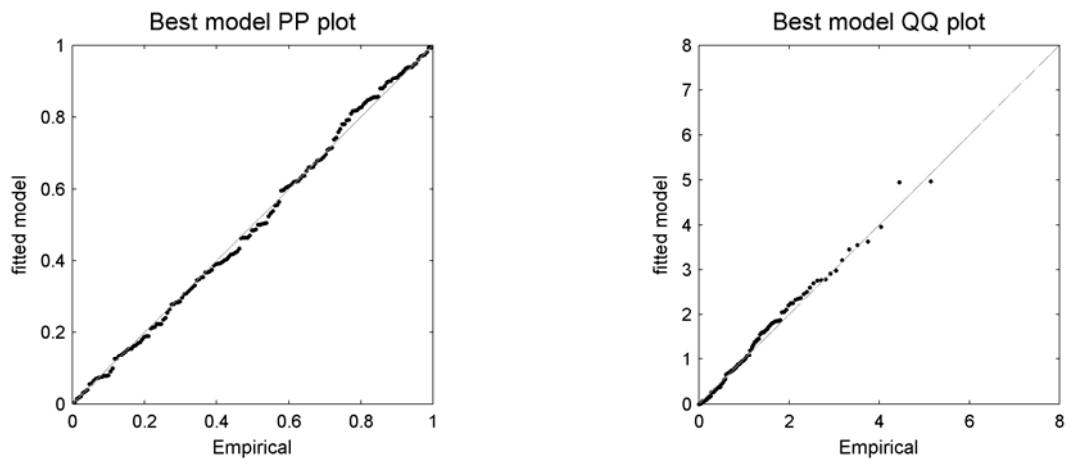
754

755

756

757

758



759

760 Figure 6. Probability (left) and quantile (right) plots for the best model $c^6 = [11.11.1.00]$

761 for the Valencia data set.

762

763

764

765

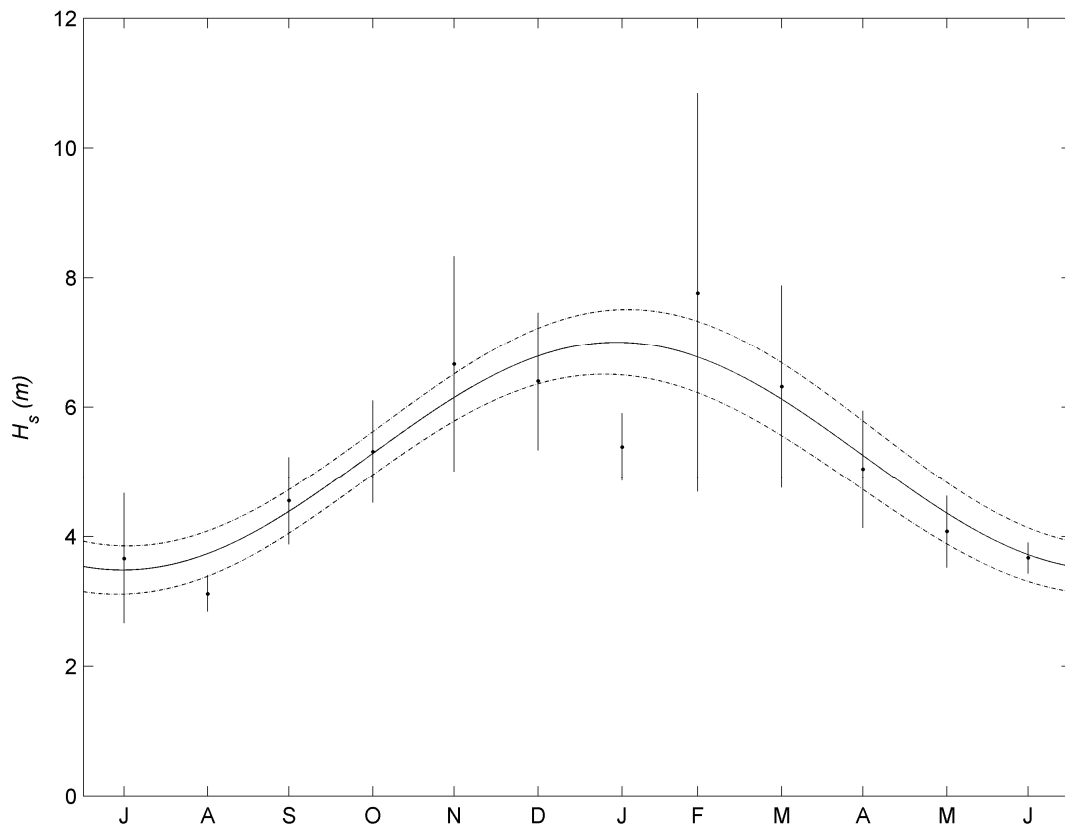
766

767

768

769

770
771
772
773
774



775
776
777
778
779
780
781
782

Figure 7. Comparison between the stationary model applied month-to-month (the midpoint are the 20-year return level and the vertical lines are the 95% confidence interval) and the time-dependent model for Bilbao data set (solid line is the 20-year return period quantile and dashed lines 95% confidence interval).

783

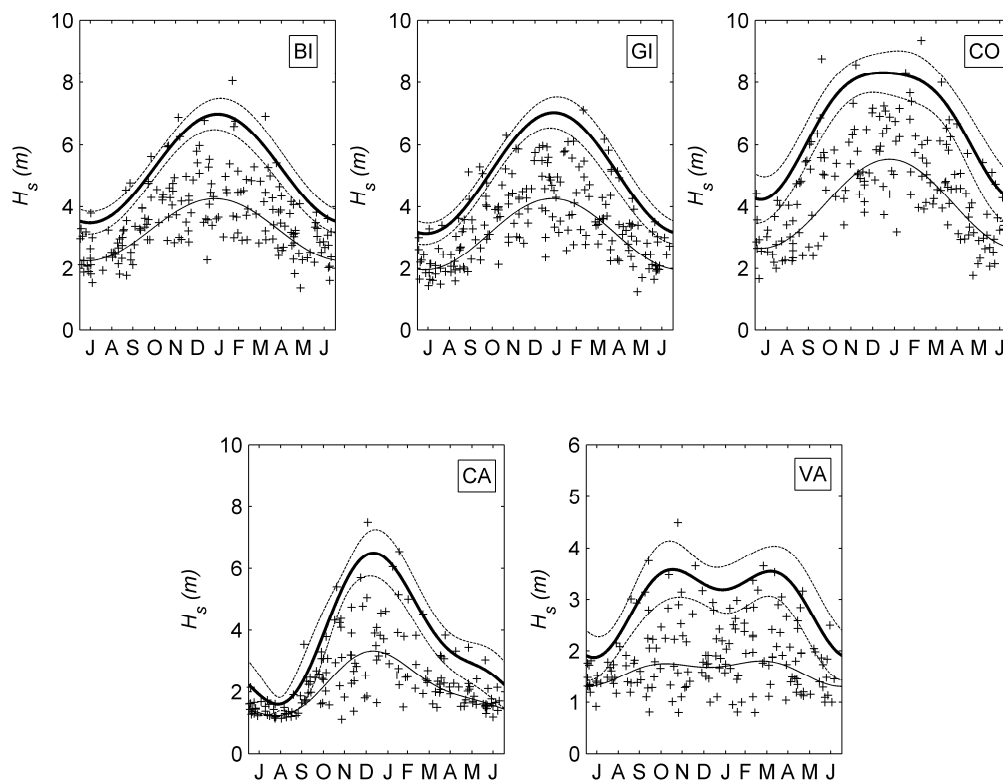
784

785

786

787

788



789

790 Figure 8. 20-year return period quantiles (bold lines) within a year and 95% confidence

791 intervals (dashed lines). The lower lines show the time-dependent location parameter.

792 Observed values of monthly maxima significant wave height indicated by crosses.

793 Results are for the best model for the five buoys.

794

795

796

797

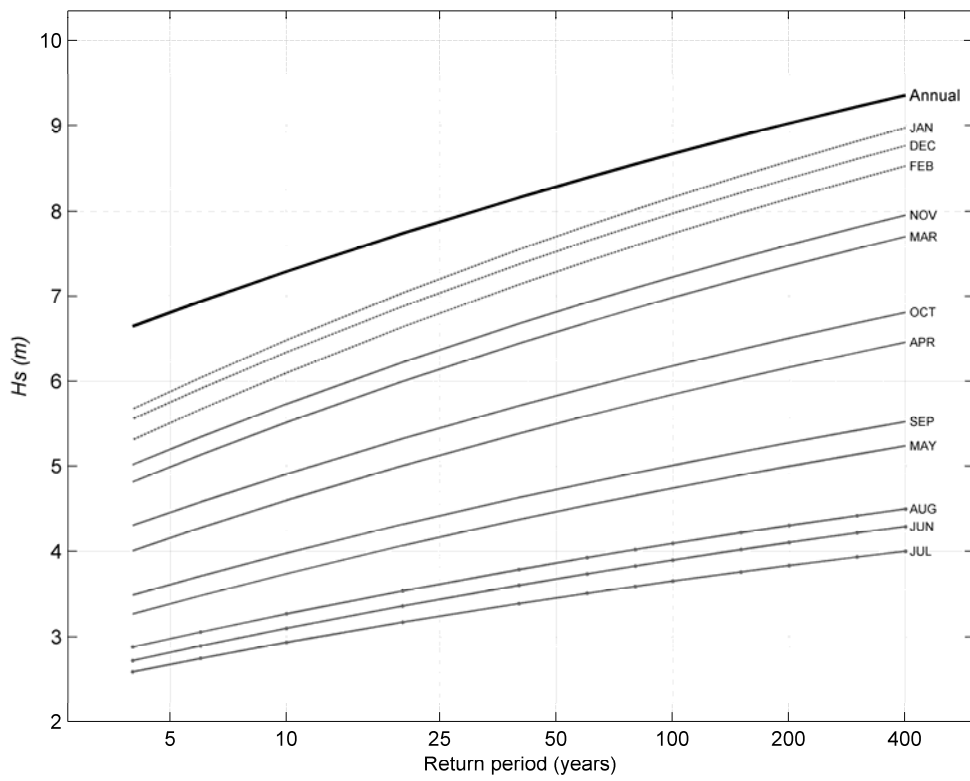
798

799

800

801

802



803

804 Figure 9. Monthly and annual return level plots for Gijon buoy.